Up-Shifted Frequency Electron-Cyclotron Current Drive in a Lower Hybrid Current Drive Plasma

T. Maekawa, T. Maehara, T. Minami, Y. Kishigami, T. Kishino, K. Makino,[a] K. Hanada, M. Nakamura,[b] Y. Terumichi, and S. Tanaka[c]

Department of Physics, Faculty of Science, Kyoto University, Kyoto 606, Japan

(Received 2 November 1992)

Using oblique injection of electron-cyclotron (EC) waves, launched from the low field side in the WT-3 tokamak, into a target plasma sustained by lower hybrid current drive (LHCD), the plasma current is ramped up at a rate corresponding to 100 kA/s. The current ramp-up is ascribed to selective EC heating of tail electrons in the LHCD plasma via fundamental EC resonance at an up-shifted frequency due to the Doppler effect.

PACS numbers: 52.35.Hr

Radio-frequency current drive has received much interest in relationship to operating a tokamak reactor in steady state [1]. Fisch and Boozer [2] predicted that electron-cyclotron (EC) waves could generate the current by preferential EC heating of electrons drifting in one toroidal direction. This scheme may be particularly suitable for control of the local current profile. Proof of EC current drive (ECCD) has been made by a number of experiments [3–9]. The current drive efficiency in these experiments was found to be low compared with that of lower hybrid current drive (LHCD) experiments. This is not surprising since the efficiency is theoretically predicted to be low for low velocity resonant electrons in a low temperature plasma. It increases rapidly with the increase of parallel velocity of the resonant electrons along the toroidal field [1,2]. In the recent experiments [8,9], the efficiency has been found to increase with the electron temperature, consistent with the theoretical analysis.

In these circumstances, it is useful to employ lower hybrid (LH) waves to boost the parallel velocity of resonant electrons for efficient ECCD. This method is interesting since the tail electrons driven by LH waves are in the energy range of ~ 100 keV, the same energy as the resonant electrons for ECCD in a high temperature reactor plasma. For these electrons, relativistic effects influence the current drive efficiency [10] as well as the EC resonance condition. Fidone *et al.* proposed ECCD in LHCD plasmas at a down-shifted EC frequency [11]. However, no current drive was observed for the injection of EC waves into LHCD discharges [12]. Although an enhancement of current ramp-up rate was observed by injection of EC waves into LHCD current ramp-up discharges, its physical mechanism was still not clear [12,13]. In this paper we present the first experimental results which show that the plasma current is ramped up by the oblique injection of up-shifted-frequency EC waves into LHCD flattop discharges.

The experiments were carried out in the WT-3 tokamak, with major and minor radii of $R_0=65$ and $a=20$ cm, respectively. The toroidal field was $B_{T0}\leq 1.75$ T at $R=R_0$. The LH waves were launched by two stacked four-waveguide arrays fed from a 2 GHz klystron with a waveguide phasing of $\Delta\phi=90°$ [14]. The EC power from a gyrotron ($\omega/2\pi=56$ GHz) was transferred through circular waveguides to a Vlasov antenna placed along the major radius. With a combination of an elliptic focusing reflector and a flat mirror for adjusting the injection angle to the toroidal direction, sharply focused EC waves were injected from the low field side in the form of a linearly polarized mode with the wave electric vector normal to the equatorial plane [15].

Figure 1 shows a typical shot of the experiments. First, the plasma current is initiated and increased to $I_P\simeq 40$ kA by the Ohmic-heating (OH) power. Second, LH waves are injected and at the same time the primary winding of the OH transformer is short circuited. Then,

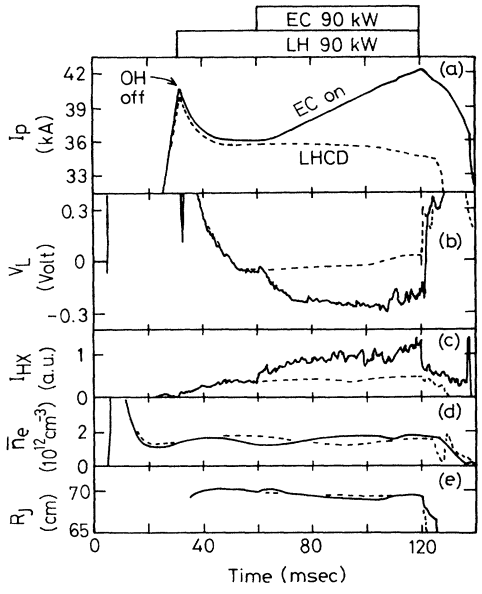

FIG. 1. Current ramp-up discharge by superposition of EC waves on a lower hybrid current drive plasma (dashed lines). (a) plasma current, (b) loop voltage, (c) hard-x-ray emission, (d) line averaged electron density, and (e) horizontal position of plasma current center. $P_{EC}\simeq 90$ kW, $P_{LH}\simeq 90$ kW, $B_{t0}=1.58$ T, $\Theta=60°$, and $\Omega_{e0}/\omega=0.79$.

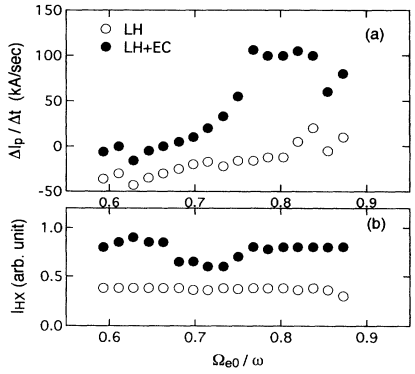

FIG. 2. Current ramp-up rate and hard-x-ray intensity vs Ω_{e0}/ω. $P_{EC}\simeq 90$ kW, $P_{LH}\simeq 90$ kW, $I_P\simeq 40$ kA, $\Theta=60°$, and $\bar{n}_e\simeq(1.5\text{-}2)\times 10^{12}$ cm^{-3}.

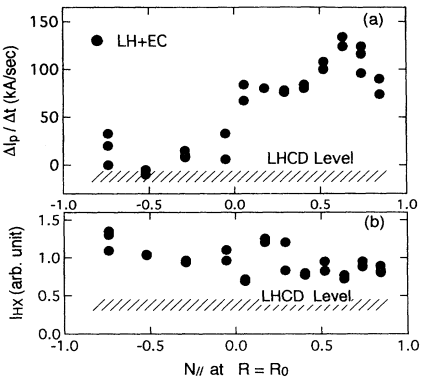

FIG. 3. Current ramp-up rate and hard-x-ray intensity vs the parallel refractive index of EC waves ($N_\parallel$) at $R=R_0$. $P_{EC}\simeq 90$ kW, $P_{LH}\simeq 90$ kW, $\Omega_{e0}/\omega=0.77$, $I_P\simeq 40$ kA, and $\bar{n}_e\simeq(1.5\text{-}2)\times 10^{12}$ cm^{-3}.

the current settles to a constant value of $I_P\simeq 36$ kA and the loop voltage measured at the cut of the vacuum vessel wall on the midplane is near zero, $V_L\simeq 0$ V. Third, EC waves are injected toward the drift direction of fast electrons in the LHCD plasma with an angle $\Theta=60°$ to the toroidal field. With this angle, the refractive index parallel to the toroidal field is $N_\parallel=0.74$ at $R=R_0$. The current is then observed to ramp up from $I_P\simeq 36$ to 42 kA at a constant rate of $\Delta I_P/\Delta t\simeq 100$ kA/s during the EC pulse. At the same time the loop voltage becomes negative ($V_L\simeq -0.25$ V) and the intensity of hard x rays (HXR) emitted from fast electrons perpendicularly to the toroidal field, I_{HX}, increases further compared with the LHCD plasma. In this case, the loop voltage at the plasma surface and at the axis of the discharge is estimated as $V_{LS}\simeq V_L-0.036$ V and $V_{L0}\simeq V_L-0.11$ V, respectively [16]. The energy range of I_{HX} is $h\nu\simeq 50\text{-}300$ keV. The bulk electron temperature ($T_e\simeq 400$ eV) measured by the soft-x-ray pulse height analysis does not change during the gyrotron pulse. The line averaged density is $\bar{n}_e\simeq(1.5\text{-}2.0)\times 10^{12}$ cm^{-3} and the horizontal position of the plasma current center is maintained at $R_J\simeq 69$ cm.

The negative loop voltage and the current ramp-up manifest increase of the poloidal magnetic field energy W_M. The increasing rate can be evaluated by a formula $\Delta W_M/\Delta t\simeq -\int_{\text{volume}} J_\parallel E_\parallel\simeq V_L I_P+L_i I_P\Delta I_P/\Delta t$, where $J_\parallel$ ($E_\parallel$) is the plasma current density (electric field) parallel to the toroidal direction, and L_i ($\simeq 0.84\,\mu$H) is the inductance inside the vessel [16]. The term $-V_L I_P$ represents the Poynting outflux from the vessel cut and $L_i I_P\Delta I_P/\Delta t$ is the time derivative of the magnetic field energy inside the vessel. The result is $\Delta W_M/\Delta t\simeq 12$ kW for the present shot of $P_{LH}\simeq P_{EC}\simeq 90$ kW. The conversion rate to the magnetic energy from the radio-frequency power $(\Delta W_M/\Delta t)/(P_{LH}+P_{EC})\simeq 7\%$ is comparable with the previous results of LHCD ramp-up experiments on ASDEX [17] and PLT [18].

Figure 2 shows the current ramp-up rate and the HXR intensity versus Ω_{e0}/ω, where $\Omega_{e0}=eB_{T0}/m$ is the EC frequency at $R=R_0$, m is the electron mass, and e the charge. The current ramp-up rate becomes optimum at $\Omega_{e0}/\omega\simeq 0.8$. Near the maximum toroidal field of WT-3 ($\Omega_{e0}/\omega\simeq 0.87$), the ramp-up rate decreases, while the HXR intensity I_{HX} does not change. Below $\Omega_{e0}/\omega\simeq 0.76$, both the ramp-up rate and I_{HX} decrease. Below $\Omega_{e0}/\omega\simeq 0.66$, I_{HX} increases again. However, no significant current drive is observed here. This range corresponds to the second harmonic resonance for relativistic fast electrons at the down-shifted EC frequency and this result is similar to the previous results in JFT-2M [12].

We varied the injection angle Θ in order to vary $N_\parallel$ of EC waves. Figure 3 shows the current ramp-up rate and the HXR intensity versus $N_\parallel$ at $R=R_0$. Here the canonical angular refractive index of EC waves, $N\psi$, is conserved due to the toroidal symmetry and the local parallel index is given by $N_\parallel=N\psi/R$ using the injection angle Θ at the flat mirror. The ramp-up rate is maximum at $N_\parallel\simeq 0.7$ and is small for the reverse injection ($N_\parallel<0$).

The relativistic EC resonance condition for the fast electrons, $\gamma[1-N_\parallel(v_\parallel/c)]=l\Omega_e/\omega$, becomes an ellipse in the electron momentum space of $\bar{P}_\parallel=m\gamma v_\parallel/mc$ and $\bar{P}_\perp=m\gamma v_\perp/mc$, where $\gamma=(1+\bar{P}_\parallel^2+\bar{P}_\perp^2)^{1/2}$ is the relativistic factor and c is the speed of light. Figure 4 shows the ellipses for the fundamental ($l=1$) and the second harmonic ($l=2$) resonance for the case of optimal current ramp-up. The accessibility condition for LH waves to reach the plasma core [$n_e(0)\simeq 3\times 10^{12}$ cm^{-3}] is $N_\parallel(\text{LH})\geq N_a=1.4$ for the present case. The condition for electrons to be resonant with these LH waves is written as $\bar{P}_\parallel\leq\gamma/N_a$ in the momentum space. Therefore, the forward fast electron tail in the LHCD plasma may be located between the circle of the bulk electron and the dashed line ($\bar{P}_\parallel=\gamma/N_a$) in Fig. 4. This tail can be resonant with the EC waves via fundamental resonance at the radial position of $R\simeq 60\text{-}70$ cm (from the axis of the

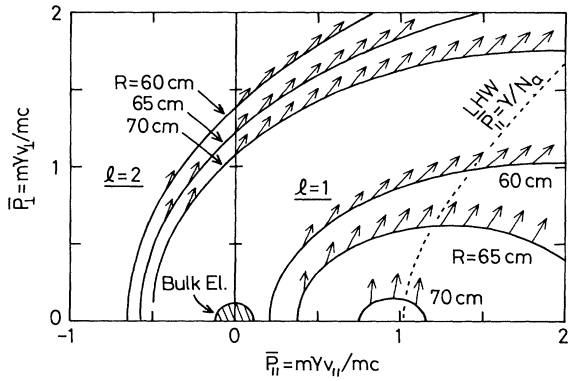

FIG. 4. Electron-cyclotron resonant ellipses for fundamental ($l=1$) and second harmonic ($l=2$) resonance in the electron momentum space for the same condition as in Fig. 1, $\Omega_{e0}/\omega = 0.79$ and $\Theta = 60°$ ($N_\parallel = 0.74$ at $R = R_0$). Dashed line denotes the boundary for electrons in resonance with LH waves with the accessibility condition of $N_\parallel(\mathrm{LH}) \geq N_a = 1.4$.

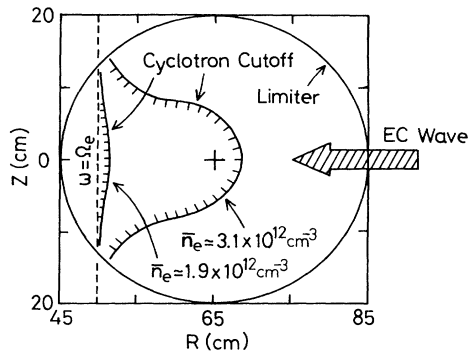

FIG. 5. Location of the cyclotron cutoff layer deduced from six-channel HCN laser interferometer data for the cases of $\bar{n}_e \simeq 1.9 \times 10^{12}$ cm^{-3} ($\Delta I_P/\Delta t \simeq 100$ kA/s) and $\simeq 3.1 \times 10^{12}$ cm^{-3} ($\simeq 20$ kA/s). $P_{EC} \simeq 90$ kW, $P_{LH} \simeq 90$ kW, $I_P \simeq 40$ kA, $\Omega_{e0}/\omega = 0.77$, and $\Theta = 60°$.

discharge to about half of the plasma radius toward inboard) as shown in Fig. 4. The arrows on the ellipses denote the direction of quasilinear diffusion for the resonant electrons. The resonant electrons gain parallel momenta in proportion to $N_\parallel$ [19]; therefore, the direction of diffusion leans forward, which is advantageous to avoid the trapped region. As Ω_{e0}/ω decreases, the fundamental ellipses disappear from the plasma core. This is consistent with the decrease of the current ramp-up rate for $\Omega_{e0}/\omega < 0.76$ in Fig. 2.

For the present oblique injection of the linearly polarized mode with $\Theta \simeq 60°$, it is calculated that 70% of the power is converted to the quasiextraordinary (QX) mode and the rest (30%) is converted to the quasiordinary (QO) mode at the plasma surface for the case shown in Fig. 1. This oblique QX mode has a significant right-hand circular component and, therefore, is strongly absorbed by the fast electrons via fundamental resonance. The numerical estimation for the present case shows that for the injection of $\Theta \sim 60°$, this mode is almost completely absorbed in the first path, while the absorption is nearly zero for the QO mode.

For injection from the low field side, this oblique QX mode may encounter the right-hand cyclotron cutoff, in which case it cannot directly reach the EC layer ($\omega = \Omega_e$) as shown in Fig. 5. It is observed that the current ramp-up rate becomes small for the density above $\bar{n}_e \simeq 2 \times 10^{12}$ cm^{-3}, and the current hardly ramps up beyond $\bar{n}_e \simeq 3 \times 10^{12}$ cm^{-3}. In the latter case, the plasma core, where the fundamental EC resonance for the LH-driven fast electron tail takes place as shown in Fig. 4, is covered with the right-hand cyclotron cutoff layer and the QX mode cannot gain access to this region. Near the maximum toroidal field, at which the ramp-up rate decreases as shown in Fig. 2, the core is also covered by the cyclotron cutoff.

For the reverse injection ($N_\parallel < 0$), Fig. 3 shows that I_{HX} increases significantly although the current ramp-up rate is small. This is not well understood. However, the following explanation is suggested. Since single pass absorption of EC waves is small, except for the forward injection of $\Theta \simeq 60° \pm 10°$, EC waves injected in the reverse direction may be absorbed via irregular multireflection at the vessel wall. As a result, both forward and backward fast electron tails could increase in a balanced manner. This would result in an increase of the HXR intensity but no appreciable increase of the total current [14].

Nearly the same current ramp-up rate is obtained for the same additional injected power by stepping up the LH power instead of the EC power. However, the incremental change of the HXR intensity is smaller compared with the EC case, suggesting that the current is carried by more energetic electrons in the EC case compared to the LH case. Figure 6 shows the energy spectra of the hard-x-ray photons emitted forward and perpendicularly to the fast electron drift direction along the toroidal field. It is important to note that the forward spectra in the EC case show a strong enhancement of the high energy photon count. These energies are beyond the cutoff range determined from the LH wave accessibility condition shown in Fig. 4, suggesting that the fast electrons are being further accelerated by the EC waves against the reverse loop voltage.

Let us consider the momentum balance of fast electrons parallel to the toroidal field. In the LHCD plasma, momentum input from the LH waves balances with friction by the bulk plasma and momentum loss via spatial diffusion. In the EC assisted, current ramp-up discharge, momentum input from the EC waves and retardation due to the reverse loop voltage contribute to the net balance. The force exerted by the reverse loop voltage is

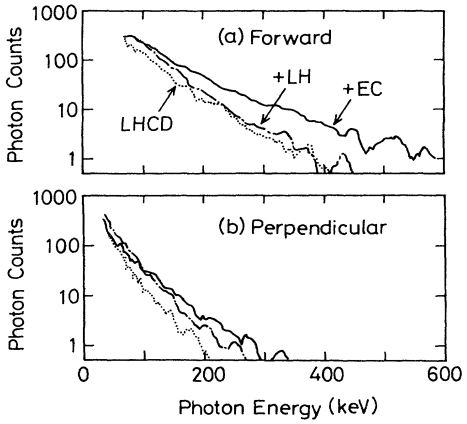

FIG. 6. Hard-x-ray energy spectra observed (a) forward and (b) perpendicular to the electron drift direction along the toroidal field for the cases of the LHCD plasma ($P_{LH} \simeq 90$ kW, $V_L \simeq -0.04$ V, $\Delta I_P/\Delta t \simeq -10$ kA/s) and current ramp-up plasmas ($V_L \simeq -0.2$ V, $\Delta I_P/\Delta t \simeq 80$ kA/s) by the superposition of LH ($+P_{LH} \simeq 90$ kW) or EC power ($P_{EC} \simeq 90$ kW). $I_P \simeq 40$ kA, $\Omega_{e0}/\omega = 0.77$, $\bar{n}_e \simeq (1.5\text{-}2) \times 10^{12}$ cm^{-3}.

$\Delta P_\parallel(\mathrm{LV})/\Delta t = -\int_{\mathrm{volume}} e n_{\mathrm{FE}} E_\parallel$, where n_{FE} is the fast electron density. Since almost all the current is carried by the fast electrons, that is, $J_\parallel \simeq -e n_{\mathrm{FE}} \langle v_\parallel \rangle$, the force is rewritten as $\Delta P_\parallel(\mathrm{LV})/\Delta t \simeq \int_{\mathrm{volume}} J_\parallel E_\parallel / \langle v_\parallel \rangle \simeq -(\Delta W_M/\Delta t)/\langle v_\parallel \rangle$, where $\langle v_\parallel \rangle$ is the average drift velocity of the fast electrons and $\Delta W_M/\Delta t$ is the time derivative of the poloidal magnetic field energy as described previously. Since the ratio of the momentum input to the energy input from the EC waves is given by $\Delta P_\parallel(\mathrm{ECW})/\Delta W(\mathrm{ECW}) = k_\parallel/\omega = N_\parallel/c$ [19], the force exerted by the EC waves may be written as $\Delta P_\parallel(\mathrm{ECW})/\Delta t = (N_\parallel/c)[\Delta W(\mathrm{ECW})/\Delta t]$. For the case of Fig. 1, $\Delta W_M/\Delta t \simeq 12$ kW; therefore, $\Delta P_\parallel(\mathrm{LV})/\Delta t \simeq -12[\mathrm{kW}]/\langle v_\parallel \rangle$. While the EC waves with $N_\parallel \simeq 0.7$ give $\Delta W(\mathrm{ECW})/\Delta t \simeq 90$ kW, therefore, $\Delta P_\parallel(\mathrm{ECW})/\Delta t \simeq 60[\mathrm{kW}]/c$. Since $\langle v_\parallel \rangle \sim 0.5c$, the EC waves have sufficient force to drive the resonant electrons against the reverse loop voltage.

Parallel momentum input for the highly collisionless electrons in a relativistic energy range above $\simeq 100$ keV improves the current drive efficiency significantly [10]. It is also advantageous to avoid the trapped region. Note that the refractive index of LH waves, $N_\parallel(\mathrm{LH}) = \gamma/\bar{P}_\parallel = c/v_\parallel$, decreases and approaches unity as the drift velocity of the resonant electrons, $v_\parallel$, increases and approaches c. Therefore, momentum input from large $N_\parallel$ EC waves (say, $N_\parallel \simeq 0.7$) becomes comparable with that from the LH waves and the ECCD efficiency approaches the LHCD efficiency for relativistic electrons. On the contrary, momentum input from EC waves is negligible compared with that from the LH waves for low energy resonance electrons, since $N_\parallel(\mathrm{LH}) = c/v_\parallel$ becomes much larger than unity. It is predicted that the ECCD efficiency is $\frac{3}{4}$ of the LHCD efficiency for this nonrelativistic energy range [2]. In order to use large $N_\parallel$ waves, we must inevitably employ the up-shifted EC frequency due to the Doppler effect. The most appropriate mode for a reactor plasma may be the oblique injection of fundamental QO mode from the low field side. This mode can propagate into the high density plasma core avoiding the cyclotron cutoff and the wave's optical depth is large enough to drive the current locally. The advantage of using an up-shifted frequency over a down-shifted frequency has been shown by a theoretical analysis [20] and a numerical simulation [21].

[a]Present address: Research Institute for Applied Mechanics, Kyushu University, Kasuga 816, Japan.
[b]Permanent address: Osaka Institute of Technology, Osaka 535, Japan.
[c]Present address: Fukui College of Technology, Sabae 916, Japan.

[1] N. J. Fisch, Rev. Mod. Phys. **59**, 175 (1987).
[2] N. J. Fisch and A. H. Boozer, Phys. Rev. Lett. **45**, 720 (1980).
[3] D. F. H. Start *et al.*, Phys. Rev. Lett. **48**, 624 (1982).
[4] M. W. Alcock *et al.*, Plasma Phys. Controlled Nucl. Fusion Res. **2**, 51 (1983).
[5] A. Ando *et al.*, Phys. Rev. Lett. **56**, 2180 (1986).
[6] H. Tanaka *et al.*, Phys. Rev. Lett. **60**, 1033 (1988); Nucl. Fusion **31**, 1673 (1991).
[7] B. Lloyd *et al.*, Nucl. Fusion **28**, 1013 (1988).
[8] R. J. James *et al.*, Phys. Rev. A **45**, 8783 (1992).
[9] V. V. Alikaev *et al.*, in *Proceedings of the Eighteenth European Conference on Controlled Fusion and Plasma Physics*, edited by P. Bachmann and D. C. Robinson (European Physical Society, Berlin, 1991), Pt. 3, p. 361.
[10] N. J. Fisch, Phys. Rev. A **24**, 3245 (1981).
[11] I. Fidone *et al.*, Nucl. Fusion **27**, 579 (1987).
[12] T. Yamamoto *et al.*, Phys. Rev. Lett. **58**, 2220 (1987).
[13] A. Ando *et al.*, Nucl. Fusion **26**, 107 (1986).
[14] T. Maekawa *et al.*, Nucl. Fusion **31**, 1394 (1991).
[15] Beam width at half power is 30 mm in the vertical direction and 60 mm in the toroidal direction at $R = R_0$ for the perpendicular injection. The launching system is depicted in K. Hanada *et al.*, Phys. Fluids B **4**, 3675 (1992).
[16] See Appendix in T. Maekawa *et al.*, Nucl. Fusion **32**, 1755 (1992).
[17] F. Leuterer *et al.*, Phys. Rev. Lett. **55**, 75 (1985).
[18] F. C. Jobes *et al.*, Phys. Rev. Lett. **55**, 1295 (1985).
[19] C. F. F. Karney and N. J. Fisch, Nucl. Fusion **21**, 1033 (1981).
[20] R. H. Cohen, Phys. Fluids **30**, 2442 (1987); **31**, 421(E) (1988).
[21] R. W. Harvey, M. G. McCoy, and G. D. Kerbel, Phys. Rev. Lett. **62**, 426 (1989).